# GROUND MOTION NEAR CAUSATIVE FAULT OF KITA–TANGO EARTHQUAKE OF 1927

S. Yoshikawa* Y.T. Iwasaki** M. Tai*** J. Matsuzaki***

SYNOPSIS

The authors describe the estimated characterists of ground motion on the base rock near the fault in the case of Kita-Tango Earthquake, occurred in south-west of Japan on March 7, 1927 (M=7.5). The ground motions at top subsurface were calculated assuming the constant particle velocity amplitude of the source spectra. The response spectral values at 11 sites with different distances from the fault are found to have good correlation with the damage ratio of the wooden house structure. The assumed base rock motion near the fault may be considered one of the possible solution to describe its character.

## INTRODUCTION:

Ground motions during earthquake has been discussed by several researchers (Seed 1968), Housner (1969), Esteva and Villaverde (1973) and Brune (1976) for engineering purposes. Most of those data are based upon the seismic records obtained at rather long distance from the epicenters. A few accelerograms have been recorded at epicentral zone by middle-sized earthquakes and are considered far from to give the complete image of near field ground motion characteristics of the large earthquakes. The present state of the knowledge on the earthquake mechanism have resulted in some success on understanding the far field seismic motion with rather long period range (Eshelby 1957, 1963), Hasket (1969), Brune (1970), Kanamori (1972), Aki (1972)). The fault motion may be simply idealized as a ramp function of displacement with time for the first order approximation in the far field from the fault zone or epicenter. However, the complex nature of the near field seismic records obtained so far have been found in doubt of such simplicity. Kita-Tango Earthquake of 1927 which is rather famous for its coseismic crustal deformation due to fault movement resulted in causing great damages of structures near fault zone. The detailed study on the damages and its distribution near the fault was tried to correlate with the characteristics of the near field ground motion associated with an earthquake of magnitude 7.5. The authors describe some efforts to understand the near field motion based upon the distribution of structural failure and the computed response spectra of the ground surface assuming input base rock motion with subsurface layered models.

* Prof., Disaster Prevention Research Inst., Kyoto Univ.
** Acting Director, Geo-Research Inst., Osaka
*** Research Staff, Geo-Research Inst., Osaka

## KITA-TANGO EARTHQUAKE:

Kita-Tango Earthquake M=7.5 (J.M.A. magnitude, Ms (surface wave magnitude)= 7.75 (Geller (1976)) occurred at the northern part of Kyoto prefecture on March 7, 1927. The epicenter was estimated as $\lambda$=135.1 E and $\psi$=35.6 N with depth of h=10km. Two faults system were found to have associated with the earthquake perpendicular to each other as shown in Figure 1. Gohmura Fault is left lateral strike slip identified as long as 18 km with its direction of NNW-SSE. Horizontal movement of the fault was found as 270cm at the maximum point. Dip component was also recognized as a heave of western block with 80cm relative to the other. Yamada Fault was 7km of length and right lateral strike slip movement of 80cm with a heave of 70cm of northern block against the other block.

Earthquake damages were reported as 12,500 wooden houses in complete collapse, 3,700 houses in burnt down and 2,900 persons in death. The great death was said due to the fire accidents followed by collapses of the houses by the ground motion. The areal distribution of the damage ratio of wooden house structure reported by Taniguchi (1927) is shown in Figure 2. The most damages were found densely concentrated near the two fault lines. Crustal displacement due to the earthquake was obtained by comparison between pre- and post-earthquake land surveys is shown in Figure 3. It was found the maximum displacement of the ground at the fault line and decreases with the distance from the fault.

## GEOLOGY OF THE AREA:

The base rock of the most part of the area is granite covered with quarternary sand and clay formations as subsurface layer except the northern part of Amino zone where the tertiary sand and mud stone formations are found below the quarternary layers. The quarternary formations are mostly alluvial soft layers deposited along the three river basins in the area. These

Fig. 1 Two fault system in Kita-Tongo Earthquake M=7.5 on March 7, 1927

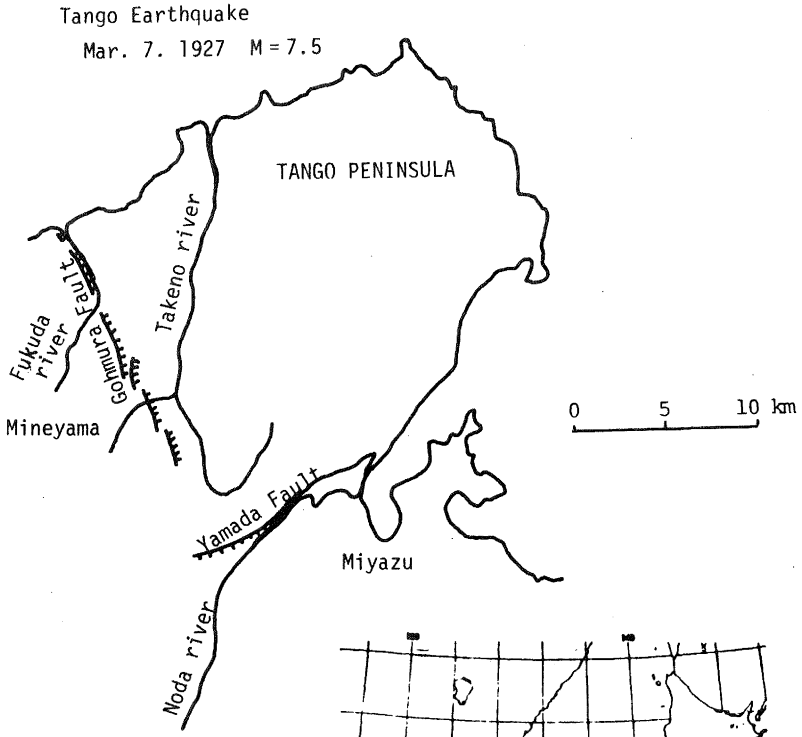


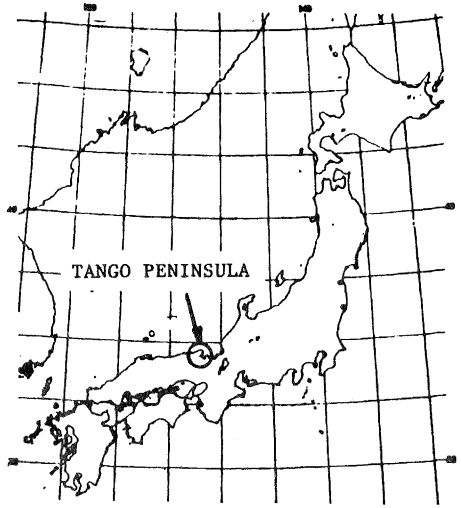


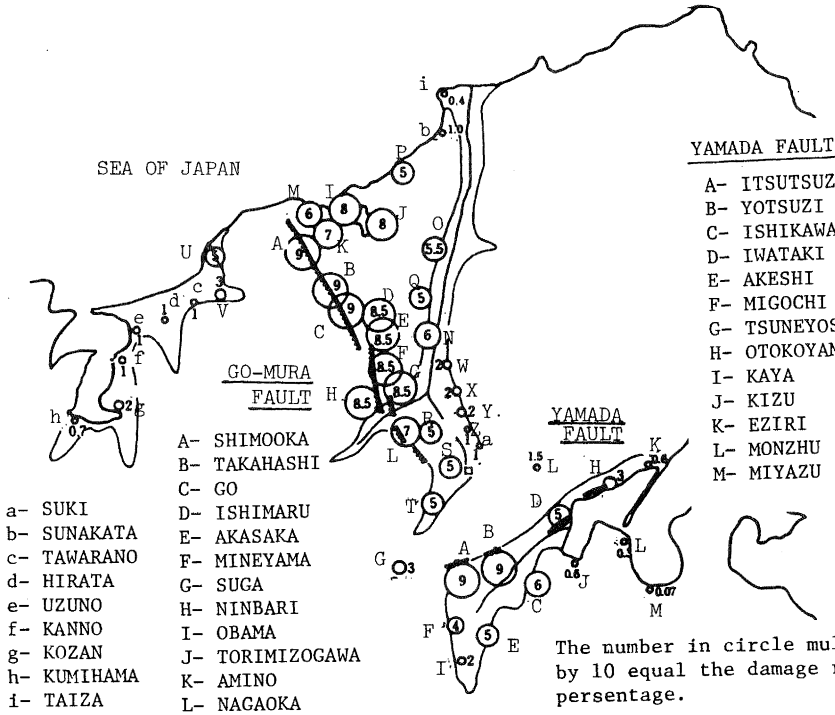


The number in circle multiplied by 10 equal the damage ratio in persentage.

Fig. 2 The distribution of the damage ratio of wooden house structure reported by Taniguchi (1927).

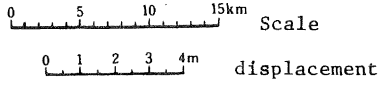


Fig. 3 Crustral displacement due to the earthquake by comparison between pre- and post-earthquake land survey by Tsuboi (1930).

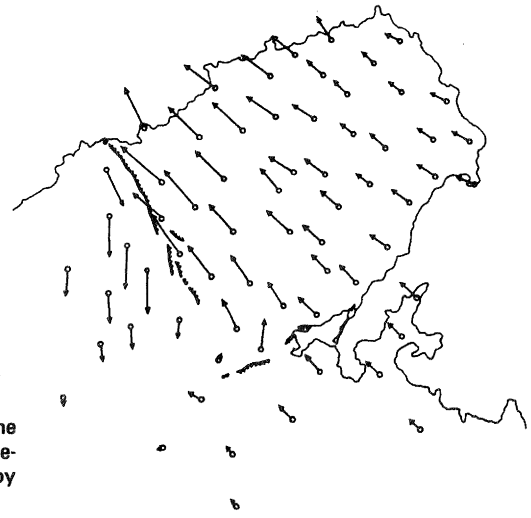

are -

1. Takeno;
2. Fukuda and
3. Noda river basins.

The structures of the sub-surface layers and its dynamic characteristics have been recognized to have great effects to the earthquake damages. The structure of the subsurface ground for the above three basins are estimated based upon the 194 boring logs. The dynamic characteristics are obtained by P- and S-waves refraction survey and micro-tremor measurements.

SUBSURFACE STRUCTURE:

The total of 194 boring logs at 69 sites which covers the most part of these three zones are used to estimate geological sections and contour line of subsurface thickness in the area. The borings logs used in this study had been obtained at the esign stages for foundations of buildings or civil engineering structures. The data contain the levels and the thickness of the subsurface layers identified based upon the terms of soil mechanics with standard penetration values. The contour line of estimated thickness of the subsurface ground is shown in Figure 4 with the village distribution in the area at the time of the earthquake. Typical subsurface geological section in each zone is shown in Figures 5 - 7 along the lines of A, B and C given in Figure 4.

The Fukuda river basin zone (Section A) has rather deep alluvium sand and clay layer as subsurface ground with thickness of 30-40 meters deposited on the tertiary sand rock formation. The surface layers are considered to be continuous but the west west part of the basin is found to have thick soft clay layer compared to the east side. In Takeno river basin, the shallow alluvium sand layer of 10m thickness covers on the granitic basa rock. S.T.P. value of the sand layer ranges from 10 to 20 of medium density. Noda river basin area is covered with loose sand, soft clay and medium dense sand layers from top surface to bottom granitic base rock.

The alluvium sand layers are divided into two different layers;

1. Very loose sand layer to S.T.P. less than 5;
2. medium dense sand layer of S.T.P. ranges from 10 to 20.

The most clay layers are found to show S.T.P. of 2 to 3. In east side of Fukuda river basin, the stiff clay of dilluvium layer is found to have S.T.P. 6 to 25.

SEISMIC REFRACTION SURVEY:

Seismic refraction survey was carried out at several sites shown in Figure 4 to obtain dynamic rigidity as well as Young's modulus of each layer, a simple shear wave source was used to generate SH-wave (horizontally polarized whear wave) for refraction survey. The results are summarized in Table 1. Comparing the seismic surveys and the subsurface geological sections, the shear wave velocity for each layer were estimated as follows;

| | |
|---|---|
| alluvium clay layer | 130-150m/sec. |
| alluvium sand layer | 140-250m/sec. |
| diluvium clay layer | 200-250m/sec. |
| diluvium sand and gravel layer | 390-400m/sec. |
| base rock (weathered) | 700-950m/sec. |

These shear wave velocities are considered for very small strain ranges of $10^{-4}$ -$10^{-5}$% and were used to represent the dynamic rigities for the subsurface layers under very small shear strain.

MICRO-TREMOR MEASUREMENTS:

Microtremors were measured at several sites where the village had been and suffered from some earthquake damages. The most villages were developed along the mountain foot sides on the alluvium ground.

The microtremors were observed at several points along a line at a site perpendicular to the mountain foot to detect any particular dynamic characteristics due to the sloping base rock condition.

The natural periods of the wooden houses typical in the area were also studied by measuring microtremors of the top floor as well as the base ground of the structure.

Power spectra of the measured microtremors were computed and are shown in Figures 8-10. The predominant frequencies of the spectra vary from 2Hz at the alluvium ground to 10Hz at the mountain foot site. THe nature of the microtremor in general is of great interest and have resulted in some discussions (The Seismic Exploration Group of Japan (1976)).

The comparison of the predominant frequencies between the field measured and the expected value computed as of shear wave multi-refraction were found in good agreement. Based upon this measured result, the microtremor in this study may be concluded as of the mode of multi-reflection. It may be further considered to have confirmed the appropriateness of the estimated subsurface sections based on boring data and its shear wave value for each layer. The effect of sloping base rock condition was found to result in only increasing frequency value with decrease of thickness of the subsurface layer.

Based upon the studies on the ground conditions in the area, 11 soil layered models were considered as appropriate to represent 27 site conditions with earthquake damages as shown in Figure

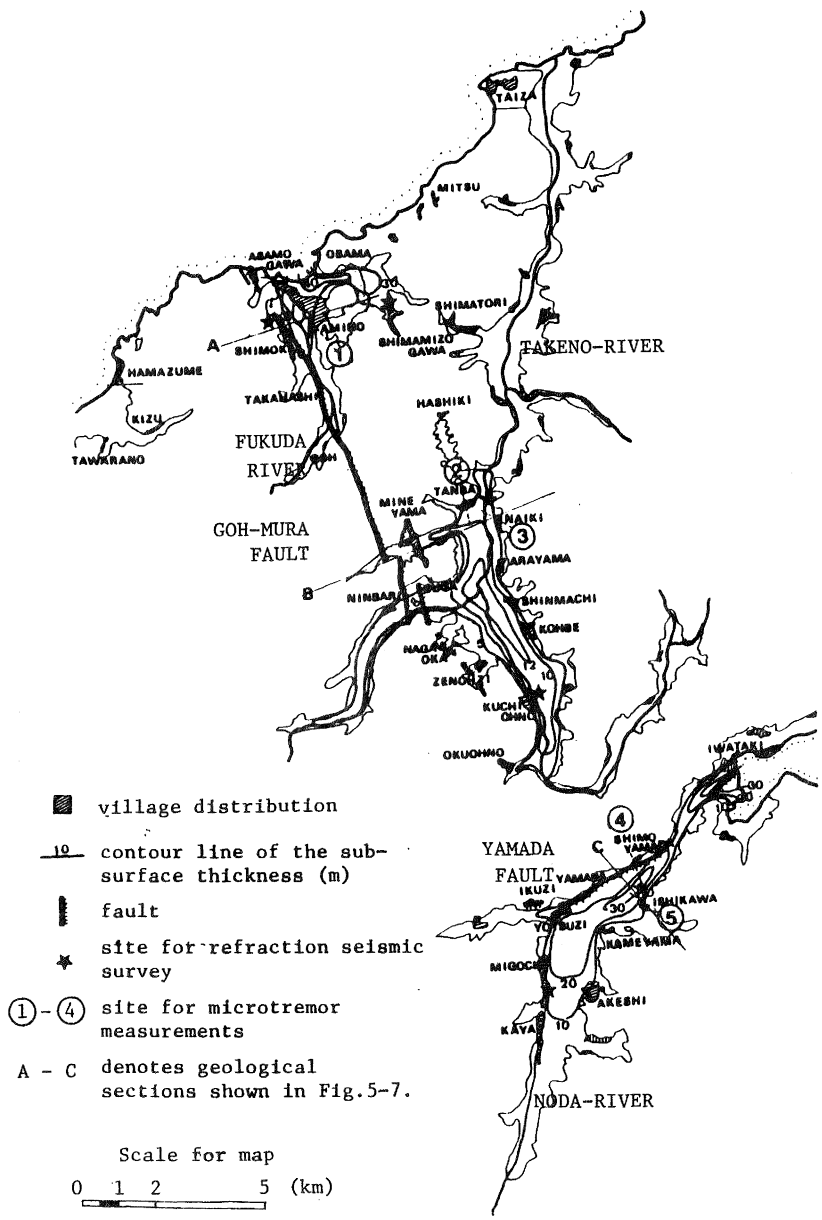


Fig. 4 Contour line of thickness of surface ground and sites of geotechnical survey

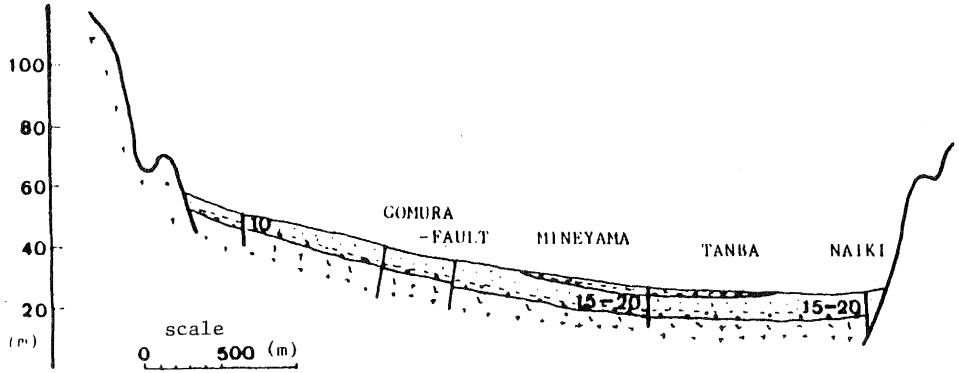


Fig. 5 Typical geological section in Fig. 4 along the line B in Takeno river basin.

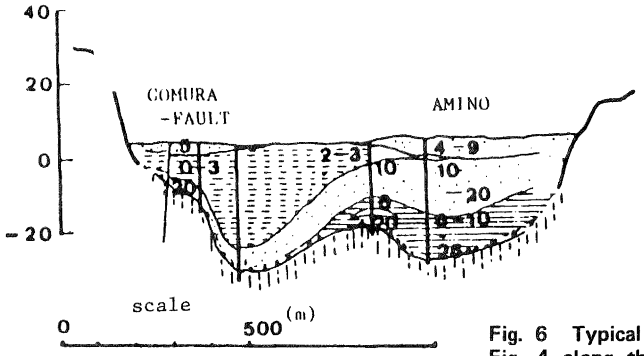


Fig. 6 Typical geological section in Fig. 4 along the line A in Fukuda river basin.

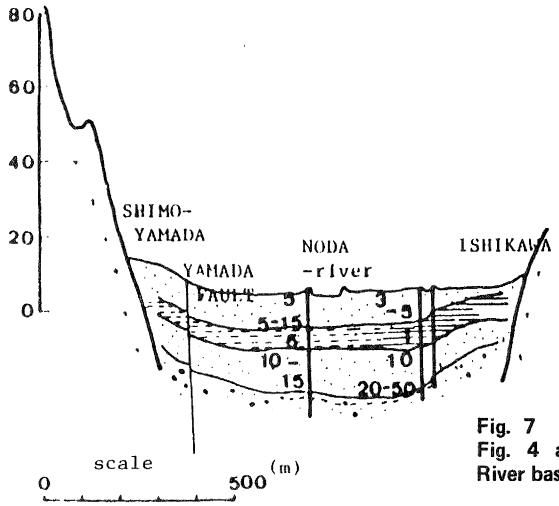


Fig. 7 Typical geological section in Fig. 4 along the Line C in Noda River basin.

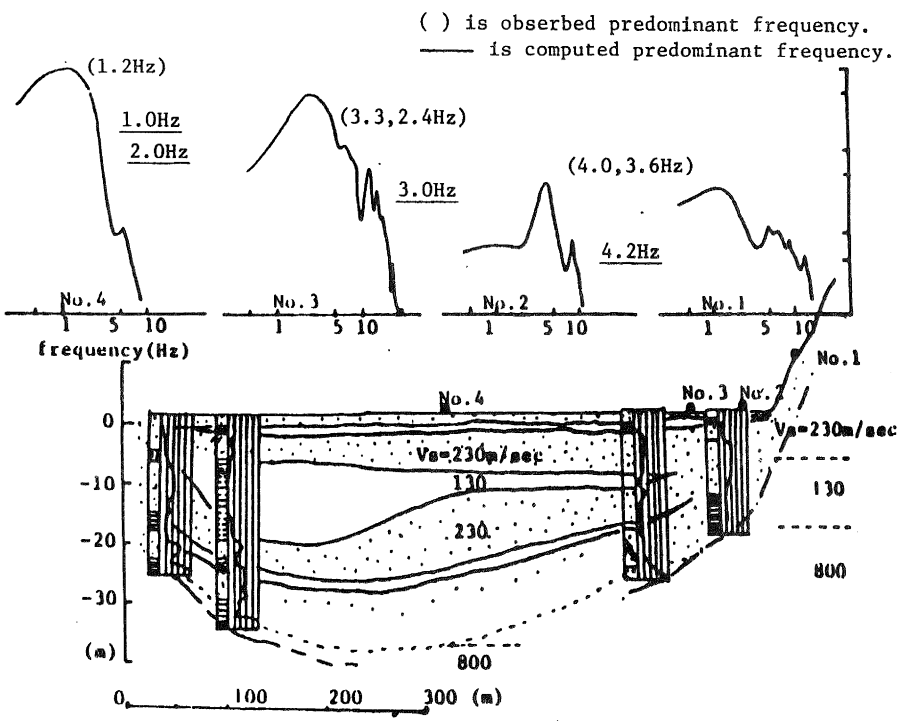


Fig. 9 Power spectra of the measured microtremors in AMINO ( 1 site, see Fig. 4).

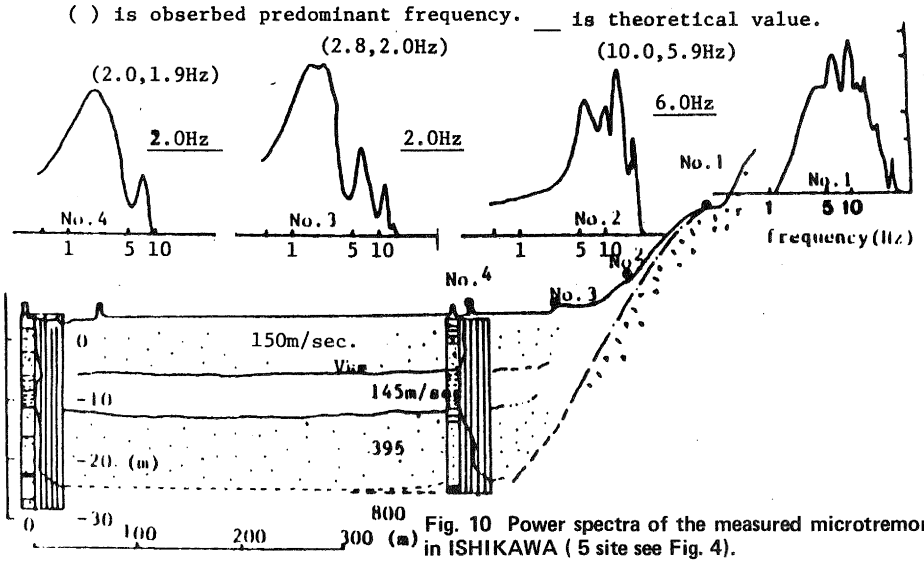


Fig. 10 Power spectra of the measured microtremors in ISHIKAWA ( 5 site see Fig. 4).

**TABLE 1 — P and S wave velocity obtained by in-situ refraction seismic method.**

(a) Noda-river, Takeno-river

| Sublayer | S -wave m/sec. | P -wave m/sec. | Poison ratio | N value |
|---|---|---|---|---|
| alluvium sand | 140 - 150 | 300 - 400 | 0.43 - 0.33 | 2 - 5 |
| diluvium sand | 390 - 400 | 1600 - 1900 | 0.47 | 20 - 50 |
| base rock weathered | 700 - 950 | 3000 - 5000 | | > 50 |

(b) Fukuda-river

| | | | | |
|---|---|---|---|---|
| alluvium sand | 210 - 250 | 440 - 530 | 0.41 - 0.26 | 10 - 20 |
| alluvium clay | 130 | 1700 - 2300 | | 2 - 3 |
| base rock (weathered) | 700 | | | > 50 |

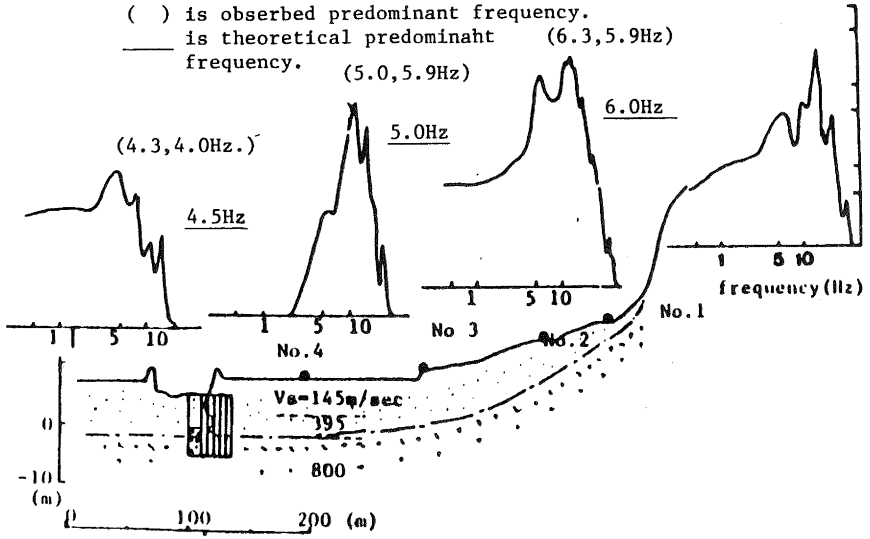


Fig. 8. Power spectra of the measured microtremors in NAIKI ( 3 site, see Fig. 4)

The natural period of the wooden houses were found to have about 0.3 sec. which is rather common value for Japanese wooden framed houses.

DAMAGES AND SUBSURFACE CONDITION

The structural damages by the earthquake was reported by Taniguchi (1927) and Kyoto pref. (1927). Those damages near the fault area may be grouped into four different types of structures as -

1. wooden house (most of them are two storey houses);
2. shrine of big wooden structure;
3. Torii structure (Gate of shrine usually made from stone columns supporting double layered horizontal stone beams and
4. textile factory of rather simple and economy type of structure.

These damages are plotted against the distance from the faults in Figure . The thickness of the subsurface layer is also shown in the lower part of the same figures. It is noted that the damages are densely distributed near the faults and rapidly decreased with the distance. In the figure, the damages are expressed by damage ratio defined as a ratio of the number of completely collapsed structures to the total number of the same kind structures in the area.

The thickness of the subsurface layers varies from 2 to 40 meters. It seems that the thickness of the layer has less effects than the distance from the faults on the earthquake damages.

The wooden houses have the natural period of about 0.3 sec. for small amplitude vibrations. However, experimental results have been reported the increase of the period from 0.3 to about 0.5 - 1.0 sec. when the structures was forced into failure under cyclic loading condition. The natural period of the shrine is estimated as much longer than that of wooden house because of the much larger wooden framed structure of shrine compared to the house. Torii is basically tall rigid structure with very short natural period. The textile firm structure was wooden one floor structure with large space and was considered to have rather long period than wooden house.

The pattern of the damage distribution with the distance from the faults were found not significantly different from each other with different natural periods. This might imply that the ground motion of this earthquake near the faults contains a wide range of frequency component to cause failure of various structures. The failure of these wooden frame structures was considered to depend on the relative displacement response value. Torii might be caused by the ground acceleration due to its rigid structures. The value of the relative displacement response to cause failure of wooden frame structure have been estimated by experimental study (Saita 1939).

7 - 10 cm initial failure of the structure;

20 cm complete collapse.

The following section describes the estimation of the base rock motion and the comparison of the change of response spectra at the top surface of the ground and the damage ratio distribution with distance from the faults.

THE ASSUMED BASE ROCK MOTION

Recent theoretical seismology have enabled the estimation of the time history of the ground motion based upon dislocation of the fault model. However, the present applicability of this approach seems to be limited within the limited frequency range. The ground motion due to body wave or surface waves with a range of period longer than a few seconds have shown good relation between the observed and the computed time histories. Seismic motions with period less than 1 sec., which are supposed to play a main role in causing damages, are considered as difficult to be estimated by simple fault movement.

Ground motion characteristics have also been described in frequency rather than in time domain. Haskel (1966) and Aki (1967) proposed the frequency spectra of ground motion at source region of earthquake based upon stochastic assumption of the fault movements.

Since the near-field motion is too complex to be expressed by a simple equation in time domain, the authors assumed possible characteristics of the motion in frequency range and used them to estimate the ground motion near the fault as a guide rule.

The particle velocity associated with shear movement in rock may be related with its shear strain as follows:

$$\nu = \gamma \times c$$

where; $\nu$ : particle velocity
$\gamma$ : shear strain
$c$ : shear wave velocity in rock

Shear wave velocity is constant in a specified rock. If the possible shear strain amplitude has its maximum value, which is usually true for rock and the value may range on the order of $10^{-4}$, the above equation says that the particle velocity is limited and has a maximum value. The shear wave velocity of the granitic base rock in the fault area may have a value of about 3000m/sec. and the shear strain at failure may be in the order of $10^{-4}$. Thus the maximum particle velocity could be estimated in the range of about 30 cm/sec.

Study of fault parameters by the

| Subsurface Ground Model | | Sites | Distance from Gohmura Fault (km) | Damage Ratio (%) |
|---|---|---|---|---|
| No. 1 | (A) | SHIMOOKA | 0 | 90 |
| 2 | (F) | MINEYAMA | 1 | 85 |
| | (H) | NINBARI | 1 | 85 |
| | (G) | SUGE | 1 | 85 |
| 3 | (K) | AMINO | 1 | 70 |
| 4 | (M) | ASMOGAWA | 1 | 60 |
| 5 | (I) | OBAMA | 2 | 80 |
| 6 | (N) | TANBA | 3 | 60 |
| 7 | (J) | TORIMIZOGAWA | 3 | 80 |
| 8 | (Q) | HASHIKI | 3 | 50 |
| | (b) | SUNAKATA | 9 | 10 |
| | (i) | TAIZA | 9 | 4 |
| 9 | (W) | NAIKI | 3 | 20 |
| | (X) | ARAYAMA | 3 | 20 |
| | (U) | HAMAZUME | 4 | 50 |
| | (V) | KIZU | 5 | 30 |
| | (O) | SHIMATORI | 5 | 55 |
| | (P) | MITSU | 5 | 50 |
| | (c) | TAWARANO | 6 | 10 |
| 10 | (g) | KOSAN | 10 | 10 |
| 11 | (d) | HIRATA | 9 | 10 |
| | (e) | UZUNO | 9 | 10 |
| | (f) | KANNO | 9 | 10 |

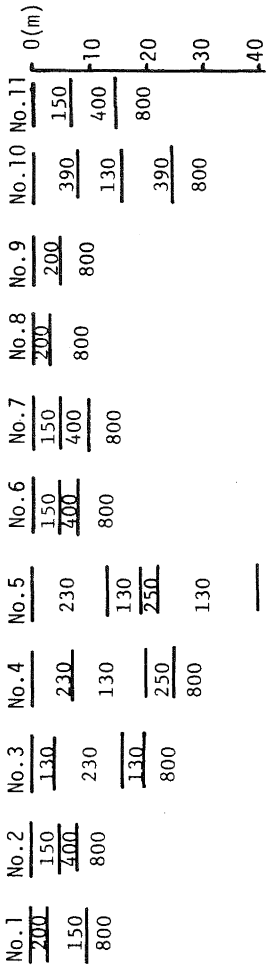


Fig. 11 Subsurface Ground Models and their applied sites with Damage Ratio

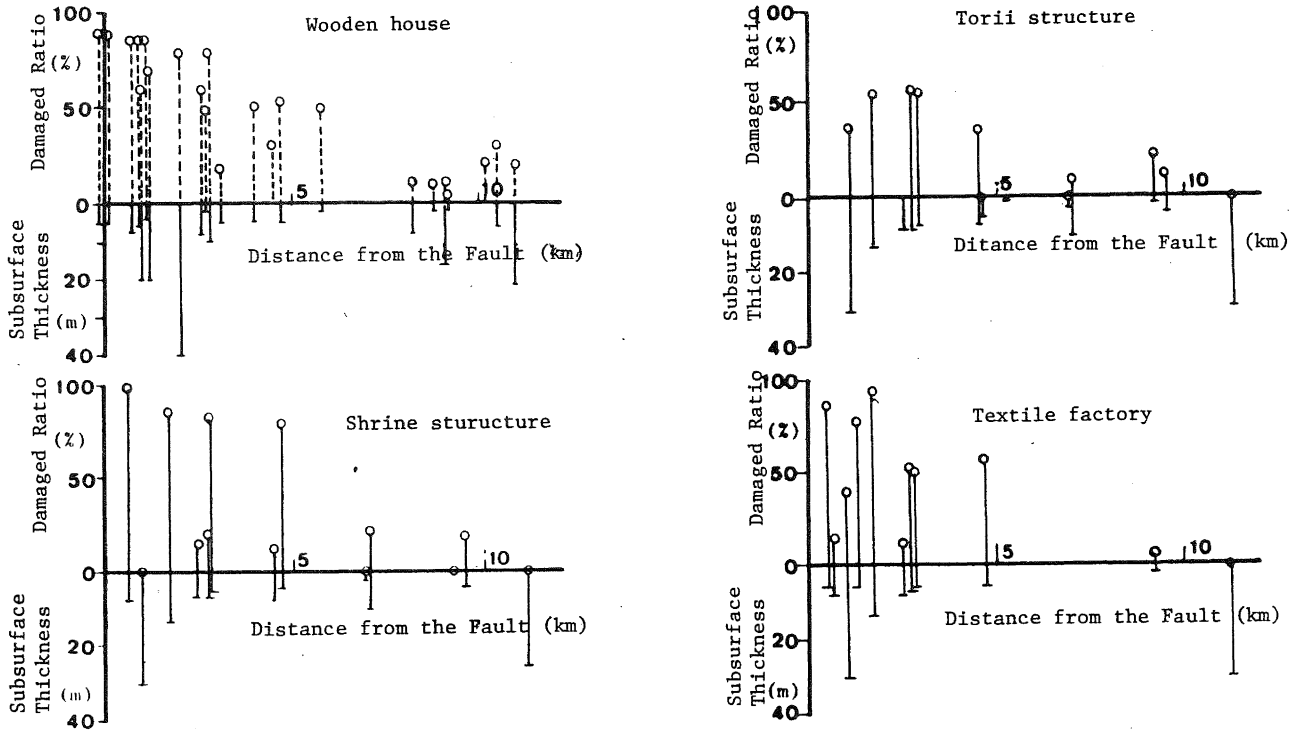


Fig. 12 The change of Damage Ratio with the distance from the fault for different structures

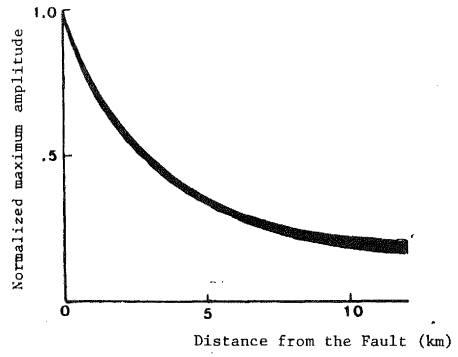


Fig. 13 Decrease of the amplitude of seismic motion with distance from the fault line based upon dislocation theory applied for Kita-Tango Earthquake

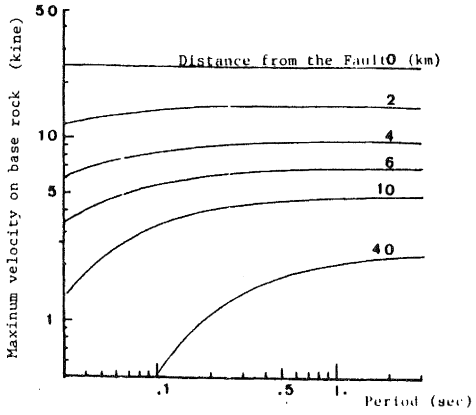


Fig. 14 Computed decrease of velocity amplitude against its period with parameters of distance from the fault.

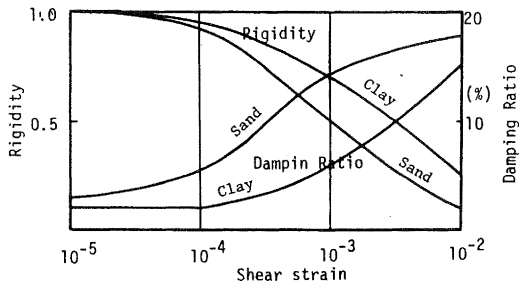


Fig. 15 Strain-dependent properties of soil.

TABLE 2 – The computed maximum accelerations at the top surface for Gomura Fault

| Site | Subsurface No. | Distance from the fault (km) | Computed Maximum Acclereation (G) | Maximum Response Displacement 0.5<T<1.0 sec. (cm) |
|---|---|---|---|---|
| MINEYAMA, MINBARI, SUGE | 2 | 1 | 1.32 | 19.9 |
| AKASAKA, ISHIMARU | 8 | 1 | 1.36 | 19.7 |
| AMINO | 3 | 1 | 0.28 | 17.4 |
| ASAMOGAWA | 4 | 1 | 0.46 | 15.5 |
| OBAMA | 5 | 2 | 0.19 | 9.07 |
| NAIKI, ARAYAMA | 9 | 3 | 1.45 | 10.9 |
| HASHIKI | 8 | 3 | 1.23 | 10.8 |
| TANBA | 6 | 3 | 1.00 | 11.5 |
| TORIMIZUGAWA | 7 | 3 | 0.99 | 11.6 |
| HAMAZUME | 9 | 4 | 1.27 | 9.2 |
| KIZU, SHIMATORI, MITSU | 9 | 5 | 1.05 | 7.5 |
| TAWARANO | 9 | 6 | 0.95 | 6.7 |
| SUNAKATA, TAIZA | 8 | 9 | 0.50 | 5.0 |
| UZUNO, KANNO | 9 | 9 | 0.73 | 5.1 |
| HIRATA | 11 | 9 | 0.46 | 5.7 |
| KOZAN | 10 | 10 | 0.20 | 14.1 |

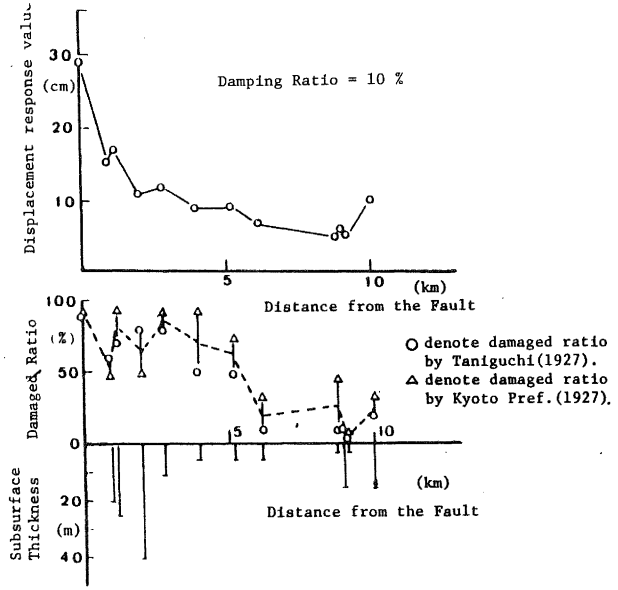


Fig. 16 The change of displacement response value and damage ratio with the distance from the fault

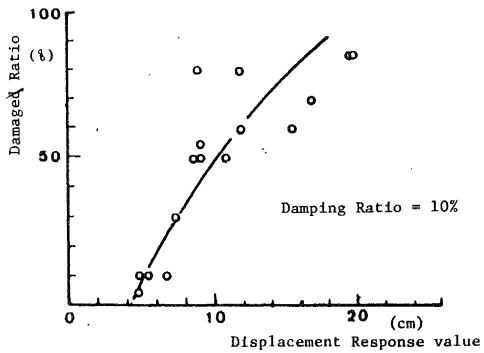


Fig. 17 Relationship between damage ratio and displacement response.

comparison of computed and recorded motions for rather long periods (Ichikawa (1971) on the Kita-Tango Earthquake showed that the toral displacement of the one side from the original position was 150 cm and the rise time required to complete the slip movement was 6 sec. resulting in a particle velocity of 25cm/sec. Considering the above results of the analysis, the particle velocity was assumed to have its spectral amplitude constant for frequency ranges concerned in the source region. This present study further assumes that the spectral amplitudes of a given frequency are those which will be computed by filtering a time history of particle velocity.

The characteristics of the base rock motion away from the fault may be obtained introducing some space radiatinal damping as well as material damping during the wave propagation applied to the constant velocity amplitude near the seismic source region. The spacial damping was assumed as the same as the decrease of the amplitude of displacement with distance from the fault which was computed by dislocation fault model applied for the Kita-Tango Earthquake. The computed amplitudes at several points away from the fault line were normalized by dividing by that of fault plane and shown in Figure . The assumed fault parameters to represent the Gohmura fault movement during the Kita-Tango Earthquake are as follows:

| | | |
|---|---|---|
| Fault dimension; | length | 36 km |
| | width | 13 km |
| Slip velocity; | 25 cm/sec. | |
| Slip displacement; | 3.0 m | |
| Rise time; | 6.0 sec. | |

The material damping was assumed as viscous characteristics expressed by Voigt model as follows;

$$\nu = \nu_0 \exp -B -R$$

where $\nu$ : particle velocity amplitude at distance R
$\nu_0$ : reference velocity amplitude at source (R=0)
$\beta$ : viscous constant (=1/2Q)
Q : quality factor
c : velocity of the seismic wave in the rock

The material damping effects on the amplitude change during wave propagation was estimated by the above equation assuming $\nu_0$ = 25 cm/sec., c = 3,000 m/sec. and Q = 200. The combined effects computed and the estimated amplitude are shown in Figure against its frequency with parameter of the distance from the fault.

The characteristics of the base rock motion is thus assumed and the base rock motion as an input to compute subsurface response was obtained by the following procedure of modifying the time history of strong motion recorded at San Fernand Earthquake.

The acceleration record of the Lake-Hughes #4 NS-component (S21W) by the San Fernand Earthquake, February 9, 1971, is thought to be appropriate to use because of the record on the rock and having the near field characteristics of the epicentral distance of 29 km. The time history of the particle velocity was computed from the acceleration record through integration. Then the amplitude change with time for a specified frequency is computed by digital filtering technique. Thus obtained amplitude history for each frequency is modified in such a way that the maximum amplitude in the time history is modified as the same amplitude as is specified in Figure 14 at a distance from the fault. The modified amplitude history for each frequency is then synthesized to compose a time history of the base rock particle velocity at the specified distance from the fault at Kita-Tango Earthquake. These computed time histories based on the Lake-Hughes #4 record were used as base rock motion to compute the response of the top of the subsurface ground.

In this study, the damaged site of only near the Gohmura fault were analysed and shown because it was thought better to make a separate analysis of the damage effects near the Gohmura as the major fault from the minor Yamada fault.

The total of 11 subsurface models to represent 27 sites shown in the preceeding section were used to simulate the earthquake ground motion by a computer programme SHAKE 3. The strain dependent characteristics of the soils were assumed that the rigidities decrease with strain increase and the damping factors increase with increase of strain as shown in Figure 15. The rididities in the figure are normalized by dividing the initial shear modulus which was determined by shear wave velocity for each sublayer.

The maximum acceleration of the assumed base rock motion was found to vary from 1.5g at the fault line to 0.23g at the distance of 10 km away from the fault. The computed maximum acceleratios at the top surface of the ground at very near fault were found as 1.4g at the ground with thickness of about 10m (Mineyama site) to 0.28g with thickness of 30m (Amino site). These computed maximum accelerations at the top surface are shown in Table 2.

Among the damages of various structures, the wooden houses were considered as appropriate to compare the reported damage ratio and the expected damage potential based upon the assumed ground motion for each site. The expected damage potential of the wooden structure was taken as the relative displacement value through the earthquake response analysis of the ground motion at top surface of each site. The maximum response value with the range of period from 0.5 to 1.0 sec. which is expected as the natural period of the wooden house at faulure under earthquake loading condition.

Displacement response values decrease with the distance from as shown in Figure 16, which are found to correspond well with the change of the reported damage ration. The general tendency of the results of the relation between the damage ratio and relative displacement response value as the damage potential were reasonably good as shown in Figure 17.

The response value of 7 - 10 cm is found to correspond to damage ratio of 40% and 20 cm and is almost 100% of the ratio, which is reasonable compared with that found for failure criteria due to cyclic loading.

The comparison of the characteristics of the computed ground motions to damage istribution along the distance from the fault could be concluded that the assumed base rock motions near the fault based upon the constant particle velocity was one of the possible solutions at the source of the earthquake.

CONCLUSION:

The summary of the present study and the conclusion obtained is as follows:

1. The Kita-Tango Earthquake was studied as one of the typical cases, to make clear the characteristics of the ground motion near the fault based upon the change of the damage distribution with the distance from the fault as well as the ground condition.

2. The particle velocity of the base rock motion was supposed to have some limited maximum value determined by the characteristics of the rock.

3. The source spectra of the earthquake motion is assumed to have a constant amplitude of the particule velocity against frequency.

4. The amplitude of the base rock motion away from the source region are considered to decrease due to space-radiating and material damping during the travel of the waves.

5. Time history of the base rock motion was obtained by modifying a record on rock site at Lake-Hugher #4 by the San Fernand Earthquake.

6. Ground conditions of the subsurface layers in the area were estimated by boring logs, seismic refraction survey and microtremor measurements.

7. The response of the computed ground motion at the top surface was found to give reasonable correspondence with the reported damage ratio of wooden house structure.

8. The assumed source spectra and the change of base rock motion near the fault is considered one of the possible solutions of the strong ground motion at Kita-Tango Earthquake.

REFERENCES:


1. Aki, K. (1972), "Scaling Law of Earthquake Source Time Function" Geophys. J.R. Astr. Soc., 31, pp 3-25.

2. Brune, J.N. (1970), "Tectonic Stress and the Spectra of Seismic Waves from Earthquake," J. Geophys. Res., 75, pp 4997-5009.

3. Brune, J.N. (1976), "The Physics of Earthquake Strong Motion, Seismic Rosk and Engineering Decisions, "Elsvier Scientific Pub. Co., NY.

4. Eshelby, J.D. (1957), "The Determination of the Elastic Field of an Ellipsoidal Inclusion and Related Problems," Proc. Roy. Soc., A241 pp 376-396.

5. Eshelby, J.D. (1963), "The Distribution of Dislocation in an Elliptial glide zone," Phys. State Sol., 3, pp 2057-2060.

6. Esteva, L. and Villaverde, B. (1973), "Seismic Risk, Design Spectra and Structural Reliability," Proc. 5th WCEE, Rome pp 2586-2597.

7. Geller, R. (1976), "Scaling Relation for Earthquake Source Parameters and Magnitude," B.S.S.A. 66, pp 1501-1523.

8. Haskel N.A. (1969), "Elastic Displacements in the Near Field of a Propagating Fault," BSSA, 59, pp 865-908.

9. Housner, G.W. (1969), "Engineering Estimates of Ground Shaking and Maximum Earthquake Magnitude," Proc. 4th WCEE, Santiago.

10. Ichikawa M. (1971), "Reanalysis of Mechanism of Earthquakes which Occurred in and Near Japan and Statistical Studies on the Nodal Plane Solutions Obtained," Geophys. Mag., 35 pp 207-274.

11. Kanamori, H. (1972), "Determination of Effective Tectonic Stress Associated with Earthquake Faulting - The Tottori Earthquake 1943", Phys. Earth Planet. Inter., 5 pp 426-434.

12. Saita, T. (1939), "Experiments in the Vibration and Destruction of a Wooden Dwelling House," Bulletin of the Earthquake Research Institute Vol. 17, pp 152-167 in Japanese.

13. Seed H.B., Idriss, I.M. and Kiefer, F.W. (1968), "Characteristics of Rock Motion during Earthquakes," EERC, Univ. of California, Berkeley, EERC-68-5, pp 23.

14. The Seismic Exploration Group of Japan (1976), "Experimental Studies on Generation and Propagation of Seismic Waves," pp 119-157, in Japanese.

15. Taniguchi, T. (1927), "Damages of Buildings in the Province of Tango due to Destructive Earthquake," Bull. E.R.I. 3, pp 133-162, in Japanese.

16. Tsuboi, T. (1930), "Investigation on the Deformation of the Earth's Crust in the Tango District connected with the Tango Earthquake of 1927. (Part 2)", Bull. E.R.I., Vol. 9.

This paper was presented at the South Pacific Regional Conference on Earthquake Engineering, Wellington, May 1979.